PARTICLE DETECTION SYSTEMS

by
Harald A. Enge*

ABSTRACT

A brief review is given of the most common nuclear particle detectors such as the gas ionization chamber, the surface barrier detector, and scintillation detectors. Some combinations of detectors are discussed with particular emphasis on heavy-ion spectroscopy. Magnetic (momentum) spectrographs and one example of a proposed energy-mass spectrograph complete the list. Some possible future trends are indicated.

1. Introduction

I have been asked to give a talk on the future of particle detection systems. I am not particularly clairvoyant and I will attempt to illuminate the subject by looking at past and present detection systems and then try to extrapolate a bit into the future. Such extrapolations can be dangerous, however. As an example I show Fig. 1, part of which is lifted from a book by C.N. Yang.[1] The original figure gave the maximum energy attained by nuclear accelerators as a function of time up to 1960. If we extrapolate this curve to year 1995 we find that the energy expected to be attained at that time is about 10^{16} eV. Assuming that we are talking about a ring accelerator with an average orbit field of B=4 tesla, the ring radius is larger than the radius of the earth. The arrangement needed is shown in the figure. Maybe we have discovered the true significance of the rings around the planet Saturn?

I shall concentrate on equipment used for the detection of charged particles emitted in nuclear reactions. The parameters we need to measure are: the mass number A, the element number Z, the kinetic energy E_k, and the reaction angle θ. The reaction angle is often determined with sufficient accuracy by the detector geometry. In high resolution experiments, however, it may be necessary either to measure the reaction angle with high precision (1 mrad) or to design means of kinematic correction into the device.

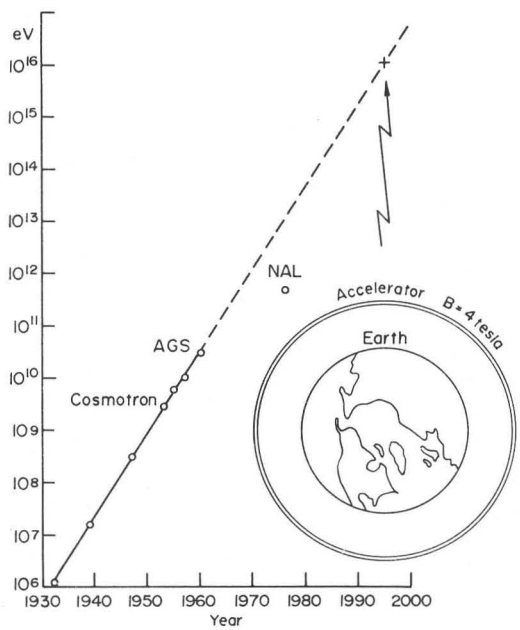

Fig. 1. Energy attained by particle accelerators vs. time. Curve up to 1960 adapted from C.N. Yang, Elementary Particles, Princeton University Press (1962).

*Department of Physics
Massachusetts Institute of Technology
Cambridge, Massachusetts 02139

2. The Gas Ionization Chamber

One of the oldest and simplest detectors for charged particles is the gas ionization chamber. For light particles its energy resolution is inferior to that of the solid state counter. For heavier ions, however, the energy resolutions of the two devices are comparable, and the ionization chamber has other distinct advantages over the solid state counter. It is therefore being used extensively again and its future looks promising. Figure 2 shows a simple ionization chamber with its cathode, Frisch[2] grid, and anode.

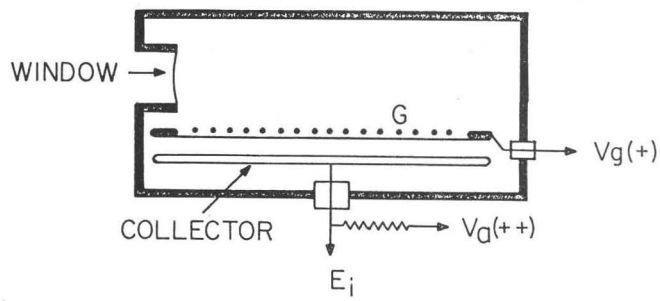

Fig. 2. A simple gas ionization detector.

The particle deposits its energy in the gas in the space between the cathode and the Frisch grid and thereby leaves a trail of ion pairs. The electrons are pulled towards the anode and reach it in, typically, a few hundred nanoseconds. The positive ions move much slower towards the cathode, and the purpose of the Frisch grid is to shield the anode from the field of the positive ions. The pulse detected at the anode is therefore directly proportional to the number of electrons collected independent of the position of the track.

The limitation on the resolution of an ionization chamber is determined by the number of ion pairs formed in the gas. The energy deposited in the gas is about 30 electron volts per ion pair. So, for instance, if the energy of the incident particle is 30 MeV, there are $N=10^6$ ion pairs formed. Naively, one then expects the resolution to be $N^{-1/2}$ or 0.1 percent. There are theoretical arguments[3] for reducing

0018-9499/79/0400-2420$00.75

this number to about 0.07 percent, but there are also other complicating factors. Typical resolution figures obtained in practice are only slightly better than 1 percent. There seems to be room for improvement in this area.

Liquid ionization chambers utilizing argon or xenon as counting medium have come into prominence lately.[4] In nuclear structure physics they may find their principal usefulness as gamma detectors.

3. Surface Barrier Detectors

The surface barrier detector (Fig. 3) is essentially a solid state ionization chamber. The basic

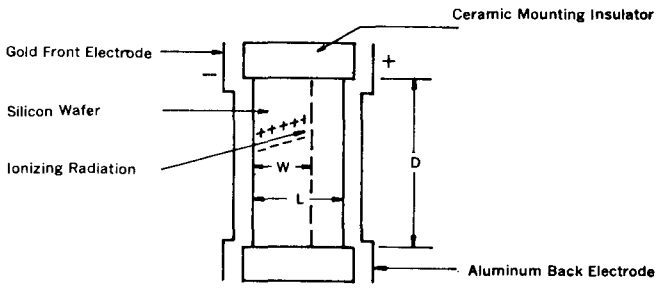

Fig. 3. Schematic of surface barrier detector (from an Ortec booklet: Silicon Surface Barrier Radiation Detectors. Instruction Manual).

material is n-type silicon. A very thin oxide layer on the surface is p-type material. The detector is therefore a diode, which when back-biased is depleted of charge carriers down to a certain depth in the n-type material. A thin layer of gold provides electrical connection to the p-type region, and an aluminum layer provides connection to the n-type material. The particle to be detected passes through the thin surface layers and deposits most of its energy in the depleted n-type material. Free charge carriers, electrons and holes, are formed and are pulled by the bias field to the aluminum and gold layers, respectively. The average energy deposited per ion pair is only 3 eV, compared to about 30 eV in the gas ionization detector. This is the main reason why the solid state ionization chamber for most applications has better resolution than the gas ionization chamber. For heavy ions the situation may be reversed, because the resolution of the solid state detector deteriorates with increasing mass number A of the particle. Eq.(1) is an empirical formula for the resolution as a function of the energy and particle type.[5]

$$\frac{\Delta E}{E} = 5\times10^{-3}\left(\frac{A}{E}\right)^{1/2}(1+0.01\,A) \qquad (1)$$

Another problem with the solid state detector is the radiation damage which increases rapidly with the element number Z of the detected particle. This makes the detector less attractive for heavy ions with high count rates.

The solid state particle detector probably has reached the limit of its capability as far as resolution is concerned. Future developments are likely to be in the direction of larger detectors, particularly position-sensitive detectors.

4. Scintillation Detectors

The scintillation counter (solid, liquid or gas) works on the principle that photons produced along the track of a particle are made to impinge upon the cathode(s) of one or more photomultiplier tubes. The output from the tube(s) is proportional to the energy deposited in the scintillator if the optical arrangement is such that the light collection efficiency is independent of where in the scintillation the track is located. The limitation on the resolution then depends upon the statistical uncertainty in the number of electrons released from the photocathode(s). This number is of the order of one electron per 300 eV deposited. The resolution is therefore generally not as good as for the ionization chamber. Figure 4 shows an example of a gas scintillation detector, and Fig. 5 is an energy spectrum obtained by this device.[6]

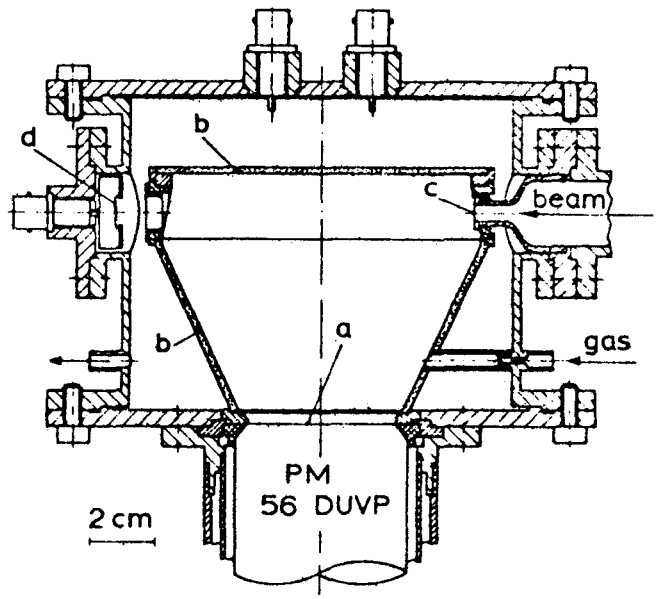

Fig. 4. Noble-gas scintillation detector. (a) multiplier window; (b) MgO reflectors; (c) 125 $\mu g/cm^2$ entrance window; (d) solid state detector. From Mutterer et al., Nucl. Instr. and Meth. 144 (1977) 159.

The advantage of the scintillation chamber over the ionization chamber is its speed. It can handle a much higher counting rate and the rise time of a pulse is about two orders of magnitude shorter, making the device more suitable for coincidence experiments. It is hard to predict the future of the scintillation counter for nuclear particles. When a large volume detector is called for it is certain to remain popular.

Table 1 lists some of the properties of the various types of detectors discussed here.

Table 1. Particle Detectors

	Typical Resol.	Rise Time	Equip. Cost	Other Features
Scint. detector	3%	1 ns	5k	High count rate
Ion. chamber	1%	100 ns	5k	Infin. Life
Surf. barr. det.	0.3%	1 ns	5k	Small, deteriorates
Magn. spectrogr.	0.03%	---	500k	Kinematic correction

0018-9499/79/0400-2421$00.75 ©1979 IEEE

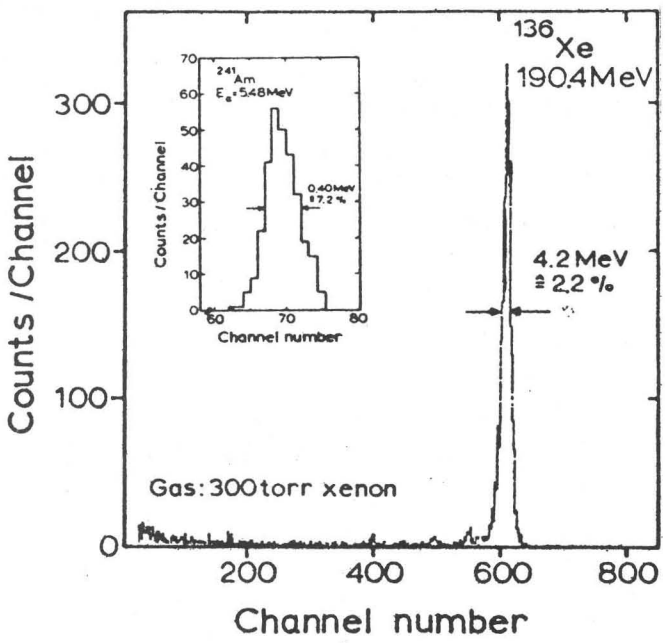

Fig. 5. Pulse height spectrum of 190.4-MeV xenon in the scintillation detector of Fig. 4.

5. Particle Telescopes

All detectors mentioned above can be used in particle telescopes generally consisting of two detectors, one thin and one thick (ΔE-E telescope). Since the energy loss ΔE in a thin absorber is a strong function of the element number Z of the particle, such a telescope can be used for determining both Z and E. Figure 6 shows an example of a telescope for heavy ions in which the front or ΔE counter is a gas ionization chamber and the back or residual E counter is a surface barrier detector.[7] Figure 7 shows a two-dimensional display of E vs. ΔE.[8] The various elements produced in the reaction are indicated on the figure. It is seen that the device gives good separation of elements at least up to Z=31.

One of the most vexing problems concerning detection techniques for heavy-ion physics is indeed Z determination. No existing ΔE-E telescope can resolve the heaviest elements. The problem is that at low and intermediate energies the difference in energy loss ΔE for two neighbor elements is too small.

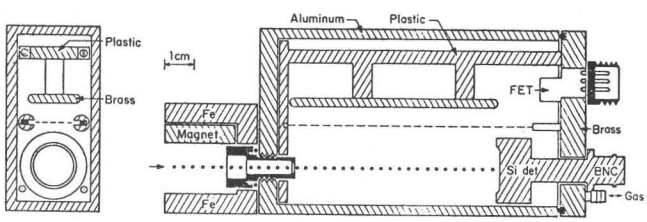

Fig. 6. Counter telescope for heavy ions. From M.M. Fowler and R.C. Jared, Nucl. Instr. and Meth. 124 (1975), 341.

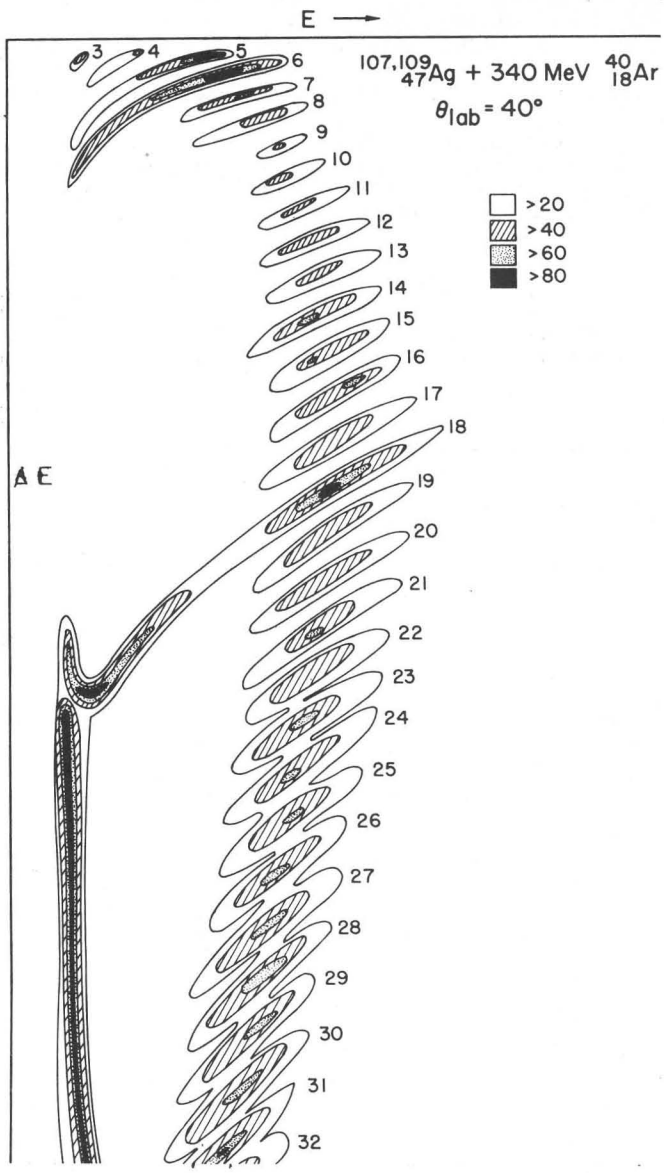

Fig. 7. Typical ΔE-E display of reaction products observed with the detector of Fig. 6 (Ref. 8).

6. Time-of-Flight Systems

Time-of-flight systems have been in use for many years as neutron energy spectrometers. They have lately become popular in heavy-ion physics for mass identification. The particle, after leaving the target, passes through a start detector and after, typically, a flight path of about a meter strikes the stop detector which records the energy as well as the arrival time. If the length of the flight path is L, the time of flight is T and the kinetic energy E, in appropriate units, the mass is simply $M=2ET^2/L^2$.

The most popular start detector is a thin carbon foil which produces a large number (>100) of secondary electrons when a heavy ion passes through. The electrons are accelerated to several keV and recorded in a solid-state detector or multiplied by a channel plate. The energy and stop detector is most often a solid-state counter. It may be preceded by a ΔE gas ioniza-

0018-9499/79/0400-2422$00.75 ©1979 IEEE

tion detector such that Z also can be determined. It is possible to determine the start and stop times to better than a fraction of a nanosecond and therefore the time resolution can be made arbitrarily good by increasing the length of the flight path. The mass resolution, however, is, of course, limited by the resolution of the E detector, and for heavy ions one percent seems to represent the state of the art.

A 600-mm^2 solid-state detector at 1 meter distance from the target represents a solid angle of 0.6 msr (millisteradians). A gas ionization detector can be made with a much larger sensitive area and about the same resolution for heavy ions. The problem is time resolution, since the ionization detector gives pulses with rise times of the order of 100 nanoseconds. A special parallel-plate proportional counter (PPPC) has been developed for this purpose at Gesellschaft für Schwerionenforschung (GSI),[9] Germany. Figure 8 shows the "Zapper,"[10] a combination stop-time, ΔE, and E detector currently being tested for use at the MIT-operated time-of-flight spectrometer at Brookhaven.

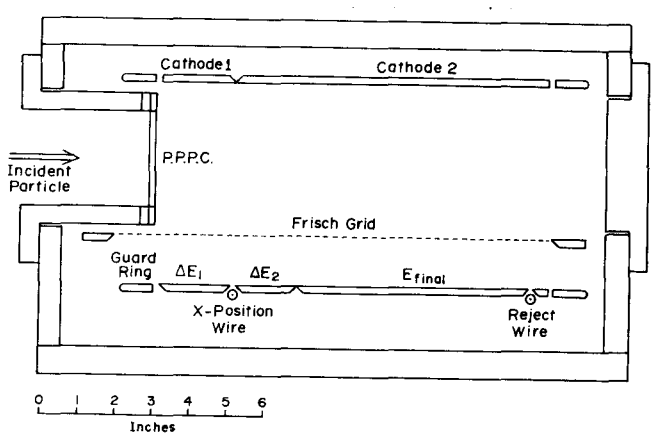

Fig. 8. The "Zapper," a stop counter for a time-of-flight system (Ref. 10).

The stop-time detector, PPPC, consists of two metalized foils about 1 millimeter apart with a gas pressure between them of, typically, 10 Torr and a voltage difference of about 700 volts, enough to produce gas multiplication. When a heavy ion passes through, the electrons released from the cathode and in the gas produce an avalanche such that an easily detectable pulse reaches the anode in relatively short time. The timing accuracy is better than 1 nanosecond.

The time-of-flight spectrometer is a very powerful instrument for heavy-ion physics. Future developments, hopefully, will include development of better energy detectors.

7. Multiparameter Systems

The trend in nuclear physics experiments is towards more and more complex setups with a number of detectors in coincidence and/or anti-coincidence. A large fraction of the experiments now being performed could not possibly have been executed without an on-line computer. Most often the setups are combinations of single detectors assembled in and around a scattering chamber. Figure 9 shows a somewhat different approach, a combination detector developed for the purpose of recording the energies and directions of

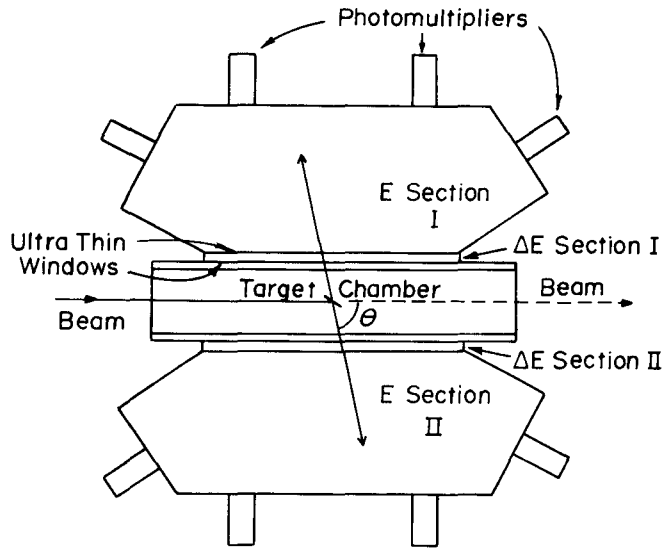

Fig. 9. The "Rat-trap," a fission-product analyzer (Ref. 11).

fission fragments of very short-lived nuclei produced in heavy-ion fusion reactions.[11] The fragment first passes through a multiwire proportional counter which records the position in the plane of the counter and hence the direction from the target. The E-counter is a gas scintillation counter, selected for its time resolution rather than for outstanding energy resolution.

8. Magnetic Spectrographs

The detectors described in the previous sections generally have resolving powers of the order of 1%. A notable exception is the surface barrier detector, but only for light ions. If a better resolving power is needed, a magnetic spectrograph is called for. The spectrograph also has other advantages such as better background rejection, less "tail" on intense peaks, possibility for blocking out intense elastic peaks -- or at zero degree -- the beam itself, possibility for making accurate kinematic corrections, etc. Magnetic spectrographs have been used for analyzing charged particles emitted in nuclear reactions since about 1947 and have evolved quite a bit since then. Table 2 shows in roughly chronological order a variety of spectrographs and their principal features.[12] The last column in the table gives a parameter Q which may be called the data-taking power of the instrument. It is defined as the solid angle Ω divided by the number of exposures needed to cover a momentum range $p_{max}/p_{min}=2$.

$$Q = \frac{\Omega \ln(p_{max}/p_{min})}{\ln 2} \qquad (2)$$

The trend of spectrograph designs has been to increase the parameter Q as well as the resolving power. Except for the increase in cost, the increase in data-taking power has been the most spectacular. Figure 10 is a graph of Q vs. time. The last point represents a heavy-ion spectrograph proposed by R. DeVries and D. Elmore and described in a report from the University of Rochester.[13] It consists of a large-aperture superconducting quadrupole followed by a superconduct-

0018-9499/79/0400-2423$00.75 ©1979 IEEE

Table 2. Single Gap Spectrographs

Spectrograph	Mean Radius R (cm)	Airgap d (cm)	Range P_{max}/P_{min}	Solid Angle Ω (msr)	Dispersion $D=\Delta x/\Delta\rho$	Magnif. M_x	M_y	D/M_x	Res. Pow.* (approx.) $\frac{R}{\Delta R}_{ab}$	Focal ψ (degrees)	Surface Shape	Kinematic Correction	Q (msr)
Annular magnet	35	1.3	1.04	0.5	2.0	1.0	---	2.0	2000	0	Straight	None	0.03
Michigan n=1/2	133		1.06	0.4	4.0	1.0	1.0	4.0	8000	55	Straight	Det. Displ.	0.03
Browne-Buechner	51	1.3	1.5	0.4	2.0	1.0	---	2.0	3000	63.5	Curved	None	0.23
Elbek	62	2.8	2.1	1.0	2.4	0.8	---	3.0	4500	45.2	Curved	Det. Displ.	1.1
Split-Pole	60	3.8	2.8	2.0	1.9	0.3	4.0	5.7	4500	41.5	Curved	Det. Displ.	3.0
Berkeley	178	10.0	1.15	1.0	2.1	0.4	5.0	5.3	5000	0	Curved	Det. Displ.	0.20
Q3DI	100	8.0	1.10	14.7	14.0	1.5	3.0	9.5	10000	43.0	Curved	Multipole	2.0
Q3DII	90	7.2	1.22	14.7	10.2	1.1	3.0	9.0	10000	43.0	Curved	Multipole	4.2
QWTH	90	7.2	1.28	10.0	7.8	1.1	4.3	7.3	10000	45.0	Straight	Multipole	3.6
QMG2	120	9.6	1.10	10.0	6.7	0.9	5.8	7.1	10000	45.0	Straight	Multipole	1.4
Indiana QDQ	135	8.0	1.03	3.2	7.7	1.0	1.0	7.7	6000	46.0	Curved	Multipole	0.14
Osaka QDDQ	150	8.0	1.06	13	11.1	1.1	4.0	10.0	10000	52	Curved	Multipole	1.1
GSI QQDQ	200	10.8	1.08-1.29	3.0	2.6-0.7	1.8-0.26	2-7	2.9-5.5	370	Variable	---	Quadrupole	.3-1.1
Jülich QQDDQ	172	6.0	1.10	10.0	9.8	0.9	7.2	11.5	?	0	Curved	Multipole	0.7
QSP Design	100	8.0	1.86	8.8	2.1	0.3	3.3	7.1	2500	38.3	Straight	Det. Displ.	7.9
Tokyo QDD	140	10.0	1.15	6.4	2.8	.38	4.4	7.4	?	55.0	Curved	Det. Displ.	1.3
IKO QDQ	180	14.4	1.10	17.2	4.6	1.2	2.5	3.9	4000	38.7	Straight	Computer	2.4
Indiana QQSP	38	5.8	1.63	<35.0	2.3	0.3	3.3	7.4	1000+	40.5	Straight	Computer	20.0
Bates QQSP	50	5.0	1.22	35.0	2.5	0.4	4.2	6.5	2000	46.1	Curved	Computer	10.0
Rochester QD	75	35	1.5	<400	---	---	---	---	3000	---	---	Computer	<200

*An approximate measure of the theoretical aberration-limited resolving power at the solid-angle listed.
+With data corrected for (x/θ^3).

ing dipole with a 40 cm gap. Two (or more) detector planes, each about one square meter, are used to trace the rays as well as measure flight times. The expected energy resolution is of the order of 0.1 percent.

Figure 11 shows another more conventional spectrograph that is only in a stage of initial optical design.[14] It has an acceptance solid angle of 35 msr and a momentum range of ±10 percent. The dispersion is intermediate between the split pole spectrograph and the Q3D spectrographs listed in Table 2, but the D/M ratio is similar.

In heavy-ion reactions it is imperative to determine the mass of the detected particles as well as their momenta. It is possible to combine the time-of-flight technique with magnetic spectroscopy for this purpose. The start-time detector should be located as close to the target as possible, where the multiple scattering in the foil has a minimum effect on the

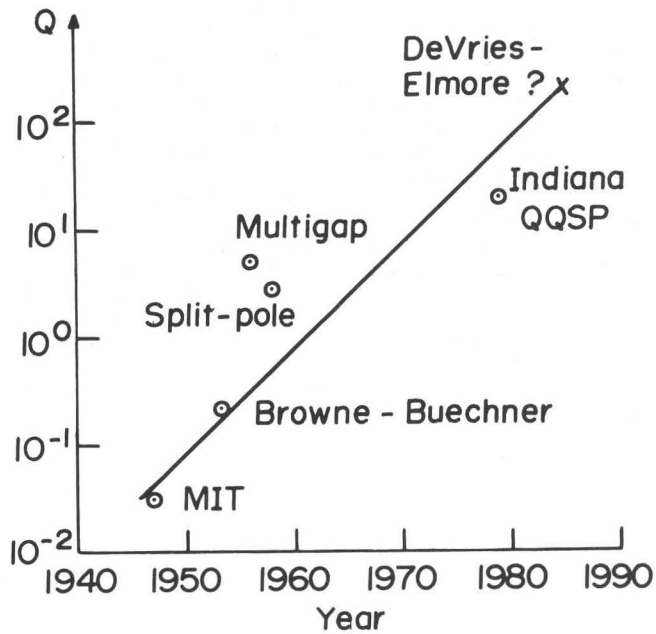

Fig. 10. Data-taking power Q (defined by Eq. (2)) vs. time.

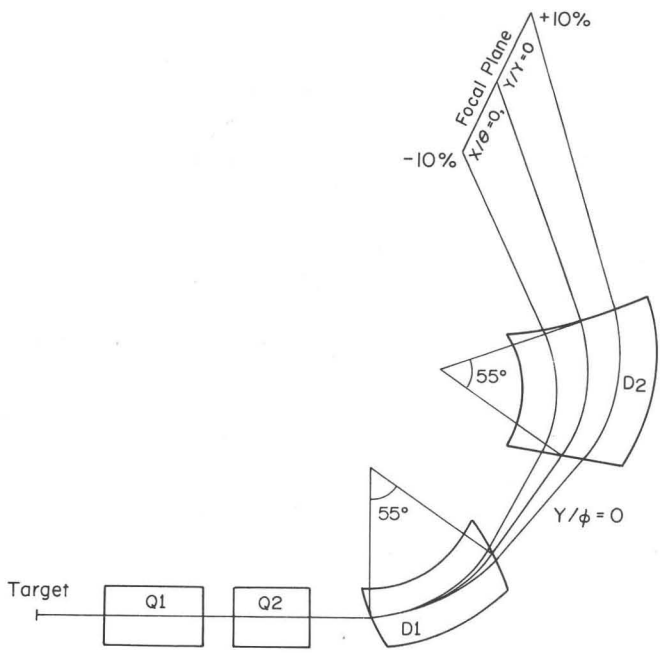

Fig. 11. A QQDD spectrograph suggested for heavy-ion work.

0018-9499/79/0400-2424$00.75 ©1979 IEEE

resolution. The focal-plane detector has to have good time resolution such that it can be used to record the stop time. There is, however, another problem associated with measuring the flight time through the spectrograph and we will analyze it in some detail. The first-order resolving power of a spectrograph is given by

$$\frac{p}{\Delta p} = \frac{DR}{M\Delta x_t} \qquad (3)$$

where D is the (non-dimensional) dispersion, M the magnification, R the layout radius and Δx_t the target spot size. A theorem by K. Brown[15] states that the D/M ratio is proportional to the integral of what Brown calls the "sine-like" function through the spectrograph. Figure 12 illustrates what is meant by that. The theorem states:

$$\frac{D}{M} = \frac{1}{RB\rho} \int (x/\theta) B \, ds \qquad (4)$$

where B is the magnetic rigidity and x/θ is the sine-like function. This last parameter describes the amplitude of a paraxial ray through the spectrograph as $x = (x/\theta)\theta$. We call the integral in Eq.(3) the Karl Brown Integral (KBI). The first-order resolving power is clearly proportional to the KBI.

It can easily be shown that the flight path difference between the two rays of Fig. 12 are also proportional to the KBI. The relationship is:

$$\frac{\Delta L}{L} = \frac{\theta}{B\rho L} \int (x(\theta) B \, ds \qquad (5)$$

where θ is defined in Fig. 12.

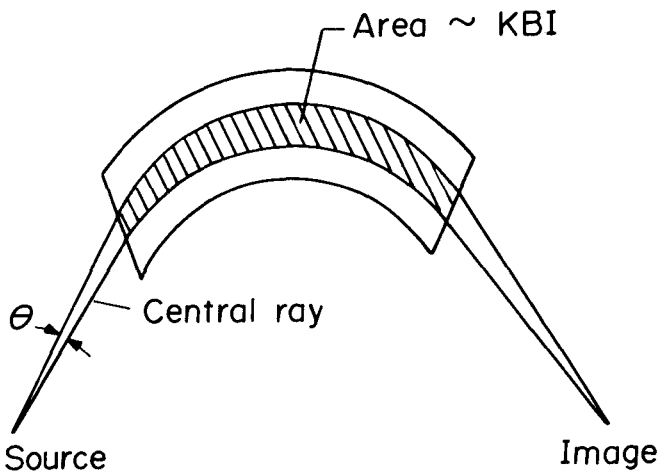

Fig. 12. The Karl Brown Integral (KBI) which determines the first-order resolving power of a spectrograph.

Combining Eqs.(4) and (5) we get

$$\frac{\Delta L}{L} = \frac{DR}{ML} \theta. \qquad (6)$$

It so happens that in modern spectrographs the factor DR/ML is close to unity. Therefore, good time resolution (i.e. mass identification) can only be obtained when θ is known to better than a few milliradians. In principle it is possible to determine θ with sufficient accuracy by measuring the angle of incidence on the focal plane, for instance by using two detector planes. In practice the angular resolution is severely affected by multiple scattering in the detector windows and gas.

Focal-plane detectors for modern particle spectrographs are most often single-wire or multiwire proportional counters. Few existing instruments record more than one coordinate, the one giving the momentum. There is a strong need for development of reliable detectors that can record two position coordinates and two direction coordinates, preferably in a single box. An interesting approach is the detector developed by W. Bertozzi and coworkers.[16]

9. Velocity Filters and Recoil Spectrographs

Time-of-flight systems for heavy-ion reactions cannot operate at zero degree or at very small reaction angles because of the ferocious intensity of elastically scattered particles. Evaporation residues from fusion reactions generally are emitted into a forward cone with a half-angle of a few degrees. Time-of-flight systems are therefore of limited usefulness for these reactions. To combat this problem, researchers at the Gesellschaft für Schwerionenforschung (GSI), Germany[17] have designed a velocity selector which filters out the beam and delivers practically only reaction products to the exit slit. It consists of two quadrupole triplets, two electrostatic deflectors and four dipole magnets, the whole system mounted permanently at 0° with the beam. A variety of experiments can be performed on the nuclei passing the exit slit: time-of-flight, alpha, beta, gamma spectroscopy, etc. The instrument has been in operation for about three years and has produced excellent results. It has been used, for instance, in a search for superheavy elements, with negative results.

A different approach was taken in the design of the Energy-Mass Spectrograph (EMS) constructed and operated by MIT at Brookhaven National Laboratory.[18,19] The instrument consists of a velocity selector deflecting vertically and a modified split pole spectrograph deflecting horizontally. The velocity can be measured with a precision of about one part in 400 and the momentum resolution is better than one part in 2000. Therefore the mass, or rather the mass/charge ratio m/q of a particle is determined with an accuracy of about one part in 400. The maximum solid angle of acceptance is 0.6 msr. As originally designed the instrument could not easily be operated at 0° because too many beam particles were scattered into the spectrograph and also the particles in the low energy tail of the beam having the correct velocity to make it through the velocity selector were flooding the detector. Therefore the instrument has been modified somewhat. A "beam trap" consisting of an electrostatic deflector followed by a magnetic deflector precedes the velocity selector proper. Because of the large difference in angle of deflection in the electrostatic deflector the beam is "peeled off" before the particles enter the velocity selector. Recent results indicate that very few high-energy beam particles, if any, make it through the instrument.

An energy-mass spectrograph with some new features is being considered for construction at the Berkeley SUPER-Hilac and at the Holifield Heavy-Ion Research Facility, Oak Ridge.[20] Figure 13 shows the optical layout of the system. The design is similar to the EMS at Brookhaven in that it deflects the particles horizontally as a function of p/q and vertically on the basis of their velocity. In zero-degree operation the main beam will be "peeled off" at the exit of the deflecting magnet D1. Further velocity selection takes place at the entrance to D2 where a vertical velocity spectrum is produced.

The solid angle of acceptance for an instrument of this kind is mostly limited by the relatively small gaps in the electrostatic deflectors combined with the need for large amplitudes to produce the desired resolution (compare the KBI discussed above). There are also other reasons why it is difficult to design an

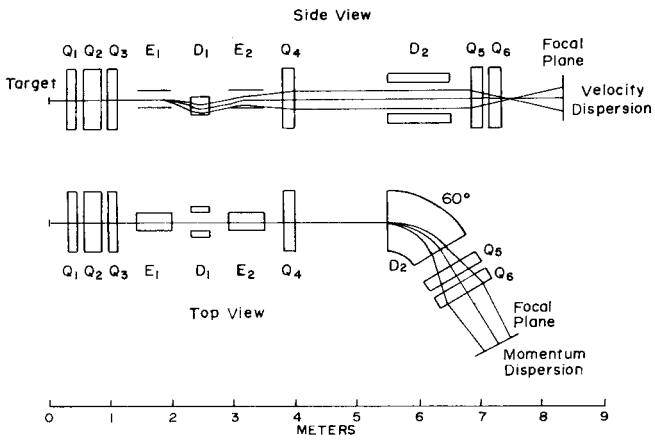

Fig. 13. An energy-mass spectrograph of novel design.

EMS with a large solid angle. First, there is no median-plane symmetry so aberration coefficients that are absent in the particle spectrograph do occur. Secondly, in addition to the parameter $\delta_p=\Delta p/p$ which occurs in magnetic optics, one needs to deal with a parameter $\delta_v=\Delta v/v$. The instrument described here has second-order corrections on both dipole boundaries and in four of the six quadrupoles. The solid angle is 3 msr; the velocity range is about $\pm$5% and the momentum range is about $\pm$10%.

10. Conclusion

The trend in nuclear detection apparatus today is towards more complex setups with multiparameter recording and towards greater data-taking power. There is a need for development of large area position sensitive detectors and for detectors with better Z-resolution as well as improved energy resolution. Gas-filled detectors obviously will play a major role in this development.

References

1. C.N. Yang, Elementary Particles, Princeton University Press (1962).

2. O.R. Frisch, unpublished report, BR-49, British Atomic Energy Project.

3. U. Fano, Phys. Rev. 72 (1947) 26.

4. C. Brassard, The Liquid Ionization Chamber, to be published in Nucl. Instr. and Meth.

5. R. Bass, J.V. Czarnecki, and R. Zitzmann, Nucl. Instr. and Meth. 130 (1975) 125.

6. M. Mutterer, J.P. Theobald, and K.P. Schelhaas, Nucl. Instr. and Meth. 144 (1977) 159.

7. M.M. Fowler and R.C. Jared, Nucl. Instr. and Meth. 124 (1975) 341.

8. J. Galin, L.G. Moretto, R. Babinet, R. Schmitt, R. Jared, and S.G. Thompson, Nucl. Phys. A255 (1955) 472.

9. G. Hempel et al., Nucl. Instr. and Meth. 131 (1975) 445.

10. U. Quade et al., Jahresbericht, Beschleunigerlaboratorium, München 1976, p. 148, and K.A. Rubin, B.Sc. thesis, M.I.T. (1978).

11. H.W. Sang, B.Sc. thesis, M.I.T. (1977).

12. H.A. Enge, Magnetic Spectrographs for Nuclear Reaction Studies, to be published in Nucl. Instr. and Meth.

13. R.M. DeVries and D. Elmore, University of Rochester Report UR-NSRL-142.

14. H.A. Enge and E.A. Enge, work in progress.

15. K.L. Brown and S.K. Howry, Stanford Linear Accelerator Report SLAC-91, p. A33.

16. W. Bertozzi, M.V. Hynes, C.P. Sargent, C. Creswell, P.C. Dunn, A. Hirsch, M. Leitch, B. Norum, F.N. Rad, and T. Sasanuma, Nucl. Instr. and Meth. 141 (1977) 457.

17. W. Faust, Gesellschaft für Schwerionenforschung MBH, Darmstadt, Report GSI-P-4-78, H. Ewald et al., Nucl. Instr. and Meth. 139 (1976) 223.

18. H.A. Enge and D. Horn, Nucl. Instr. and Meth. 145 (1977) 271.

19. M. Salomaa and H.A. Enge, Nucl. Instr. and Meth. 145 (1977) 279.

20. M. Nitschke, J. Chervenak and H.A. Enge, work in progress.

0018-9499/79/0400-2426$00.75